Supporting Information

On the mechanistic complexity of oxygen evolution: Potential-dependent switching of the mechanism at the volcano apex

Kai S. Exner[1,2,3,*]

[1] *University Duisburg-Essen, Faculty of Chemistry, Theoretical Inorganic Chemistry, Universitätsstraße 5, 45141 Essen, Germany*

[2] *Cluster of Excellence RESOLV, Bochum, Germany*

[3] *Center for Nanointegration (CENIDE) Duisburg-Essen, Duisburg, Germany*

* Corresponding author: kai.exner@uni-due.de ORCID: 0000-0003-2934-6075

Keywords

oxygen evolution reaction; reaction mechanism; volcano plot; descriptor approach; potential-dependent changes

1 Volcano plot for *U* = 1.23 V *vs*. RHE

Figure S1 indicates the raw data for the OER volcano plot at U = 1.23 V *vs*. RHE, and its analysis culminates into **Figure 2a** of the main text.

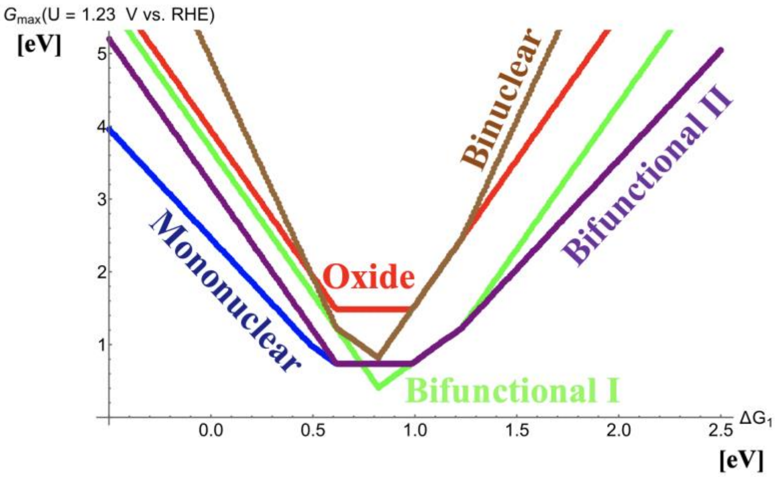

Figure S1. Potential-dependent volcano plot for the mononuclear (blue), bifunctional I (green), bifunctional II (purple), binuclear (brown), and oxide (red) mechanisms of oxygen evolution at U = 1.23 V *vs*. RHE. In case that data points are not visible, they overlap with another volcano curve. To derive the volcano lines, the activity measure $G_{\max}(U)$ (cf. equation (41) in the Methods section) is evaluated for the intermediate states of all mechanistic pathways (cf. equations (36) – (40) and (42) – (67) in the Methods section) in dependence of the descriptor ΔG_1, which is varied between –0.5 eV and +2.5 eV in steps of 0.01 eV. In the analysis, the following scaling relations are taken into account: $\Delta G_2 + \Delta G_3 = 3.20$ eV and $\Delta G_2 = 2 \times \Delta G_1$.

2 Volcano plot for SRI = 3.00 eV

Given that smaller scaling-relation intercepts (SRI) than the conventional value of 3.20 eV have been reported in the literature **[1-3]**, OER volcano plots adopting SRI = 3.00 eV are derived. The results are compiled in **Figures S2-S3**.

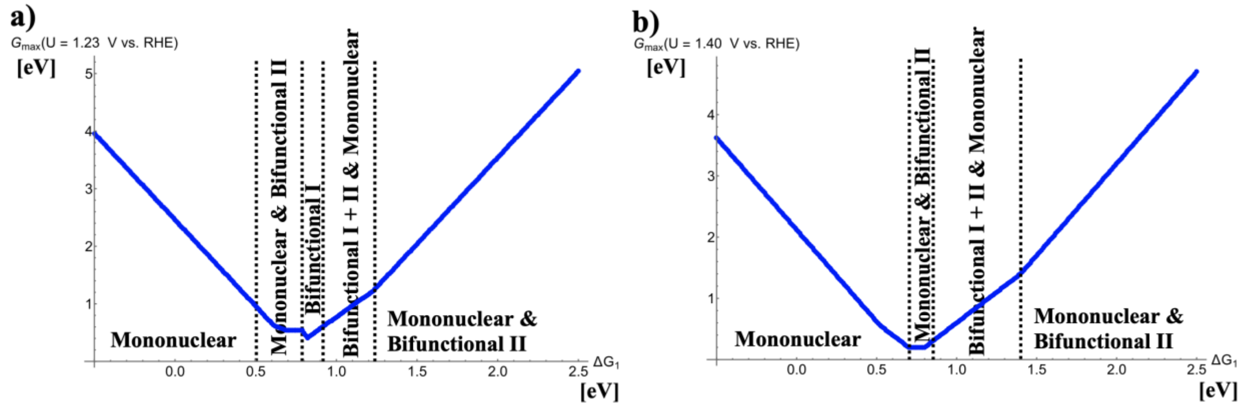

Figure S2. Potential-dependent volcano plots for various pathways of the oxygen evolution reaction at **a)** U = 1.23 V *vs*. RHE and **b)** U = 1.40 V *vs*. RHE. The energetically favored mechanisms in the approximation of $G_{max}(U)$ as a potential-dependent activity measure are indicated in dependence of the adsorption free energy of the *OH intermediate, ΔG_1. To derive the volcano curves, the following scaling relations are taken into account: $\Delta G_2 + \Delta G_3 = 3.00$ eV and $\Delta G_2 = 2 \times \Delta G_1$.

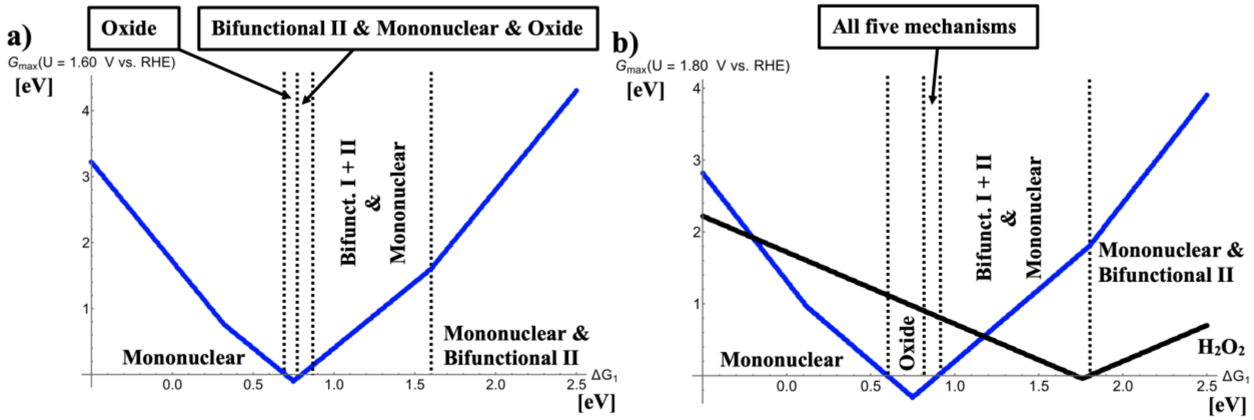

Figure S3. Potential-dependent volcano plots for various pathways of the oxygen evolution reaction at **a)** U = 1.60 V *vs*. RHE and **b)** U = 1.80 V *vs*. RHE. The energetically favored mechanisms in the approximation of $G_{max}(U)$ as a potential-dependent activity measure are indicated in dependence of the adsorption free energy of the *OH intermediate, ΔG_1. The black volcano curve in panel **b)** refers to the two-electron water oxidation with H_2O_2 as the main product. To derive the volcano curves, the following scaling relations are taken into account: $\Delta G_2 + \Delta G_3 = 3.00$ eV and $\Delta G_2 = 2 \times \Delta G_1$.

Compared to **Figures 2-3** of the main text (SRI = 3.20 eV), there are minor alterations in terms of the preferred OER mechanism. For instance, the bifunctional I mechanism does not govern the volcano apex at U = 1.40 V *vs*. RHE, but rather the mononuclear and bifunctional II pathways are found to be favored. Yet, the general picture in terms of the mechanistic complexity at the volcano apex is not changed when the SRI is reduced to smaller values. Also, it appears that the volcano legs are described by the same mechanisms as it is the case for SRI = 3.20 eV (cf. **Figures 2-3**). This finding underpins the robustness of the presented analysis despite the assumption of scaling relations in the evaluation of adsorption free energies.

3 Sensitivity analysis of the *OH *vs*. *O scaling relation

While the scaling relation between the *OH and *OOH intermediates is quite robust (cf. equation (34) in the Methods section), the opposite case is observed for the scaling relation between the *OH and *O adsorbates (cf. equation (35) in the Methods section). This is the reason why a sensitivity analysis is executed to demonstrate that the observed OER volcano trends hold true even if the energetics of the *OH and *O intermediates is altered to a reasonable extent. While **Figures S4-S5** compile volcano curves for an enlarged slope ($\Delta G_2 = 2.3 \times \Delta G_1$), **Figures S6-S7** indicate the opposite scenario of a reduced slope ($\Delta G_2 = 1.5 \times \Delta G_1$) between the free energies ΔG_2 and ΔG_1.

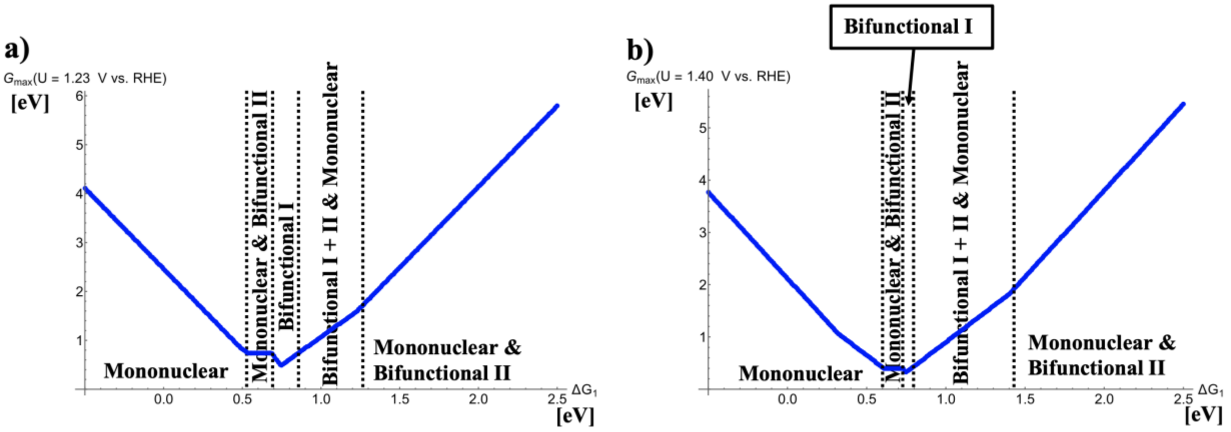

Figure S4. Potential-dependent volcano plots for various pathways of the oxygen evolution reaction at **a)** $U = 1.23$ V *vs*. RHE and **b)** $U = 1.40$ V *vs*. RHE. The energetically favored mechanisms in the approximation of $G_{\max}(U)$ as a potential-dependent activity measure are indicated in dependence of the adsorption free energy of the *OH intermediate, ΔG_1. To derive the volcano curves, the following scaling relations are taken into account: $\Delta G_2 + \Delta G_3 = 3.20$ eV and $\Delta G_2 = 2.3 \times \Delta G_1$.

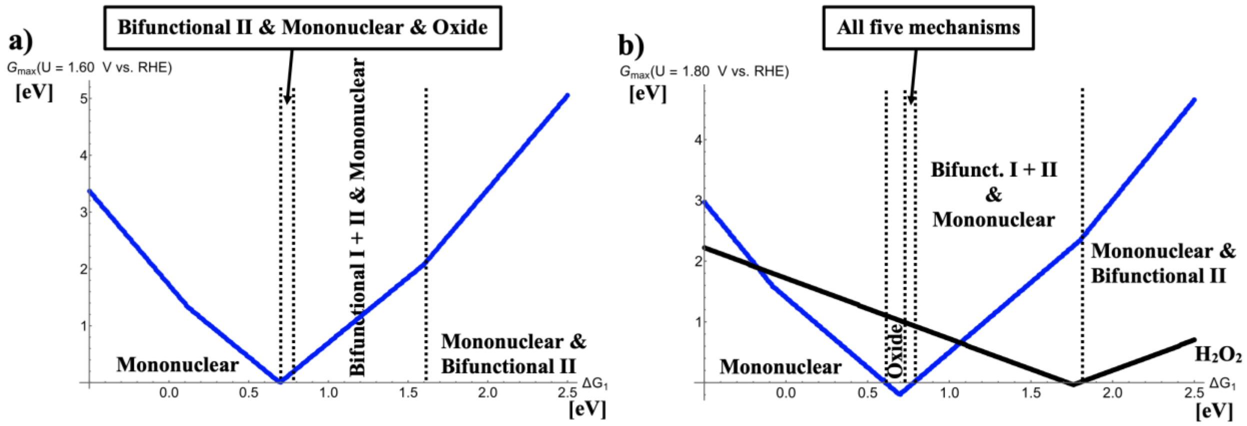

Figure S5. Potential-dependent volcano plots for various pathways of the oxygen evolution reaction at **a)** $U = 1.60$ V *vs*. RHE and **b)** $U = 1.80$ V *vs*. RHE. The energetically favored mechanisms in the approximation of $G_{max}(U)$ as a potential-dependent activity measure are indicated in dependence of the adsorption free energy of the *OH intermediate, ΔG_1. The black volcano curve in panel **b)** refers to the two-electron water oxidation with H_2O_2 as the main product. To derive the volcano curves, the following scaling relations are taken into account: $\Delta G_2 + \Delta G_3 = 3.20$ eV and $\Delta G_2 = 2.3 \times \Delta G_1$.

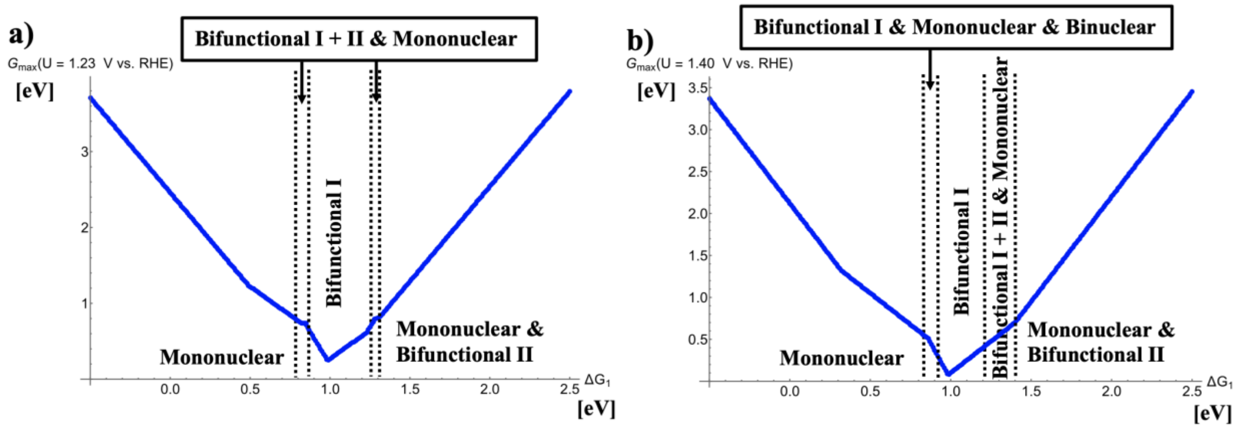

Figure S6. Potential-dependent volcano plots for various pathways of the oxygen evolution reaction at **a)** $U = 1.23$ V *vs*. RHE and **b)** $U = 1.40$ V *vs*. RHE. The energetically favored mechanisms in the approximation of $G_{max}(U)$ as a potential-dependent activity measure are indicated in dependence of the adsorption free energy of the *OH intermediate, ΔG_1. To derive the volcano curves, the following scaling relations are taken into account: $\Delta G_2 + \Delta G_3 = 3.20$ eV and $\Delta G_2 = 1.5 \times \Delta G_1$.

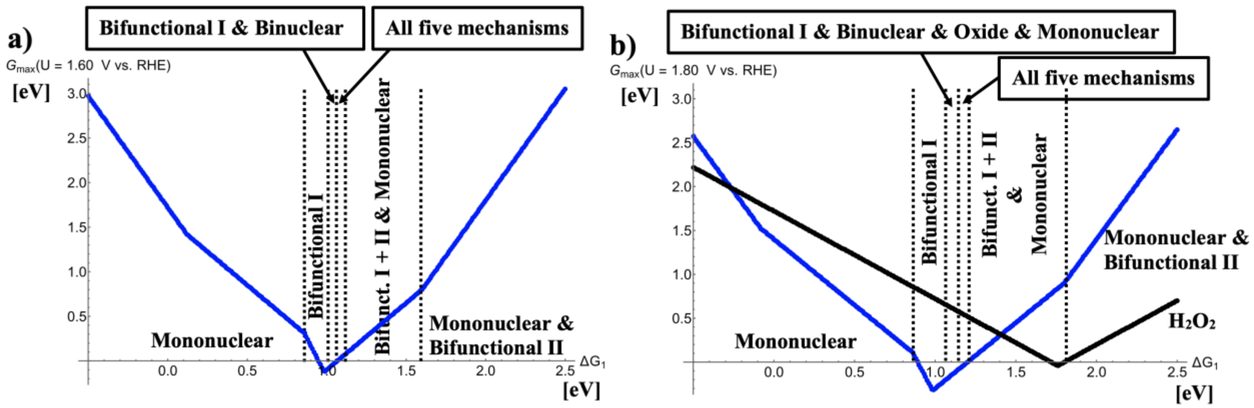

Figure S7. Potential-dependent volcano plots for various pathways of the oxygen evolution reaction at **a)** $U = 1.60$ V *vs*. RHE and **b)** $U = 1.80$ V *vs*. RHE. The energetically favored mechanisms in the approximation of $G_{\text{max}}(U)$ as a potential-dependent activity measure are indicated in dependence of the adsorption free energy of the *OH intermediate, ΔG_1. The black volcano curve in panel **b)** refers to the two-electron water oxidation with H_2O_2 as the main product. To derive the volcano curves, the following scaling relations are taken into account: $\Delta G_2 + \Delta G_3 = 3.20$ eV and $\Delta G_2 = 1.5 \times \Delta G_1$.

Figures S4-S7 confirm that the volcano legs of the OER volcano are mainly governed by the mononuclear or the mononuclear and bifunctional II descriptions for strong and weak bonding of *OH, respectively. This finding coincides with the volcano plots of the main text (cf. **Figures 2-3**). At the volcano apex, a slightly different situation is observed in that the various mechanisms benefit either from an enlarged slope (cf. **Figures S4-S5**) or a reduced slope (cf. **Figures S6-S7**) between the free-energy changes ΔG_2 and ΔG_1. For instance, the reduced slope is beneficial for the bifunctional I mechanism in that it becomes favored at the volcano apex, independent of the amount of overpotential applied (cf. **Figures S6-S7**). However, a deviation of the slope by 0.5 from the original scaling relation, $\Delta G_2 = 2.0 \times \Delta G_1$, is quite severe. As discussed in reference **[4]**, deviations in the order of 0.3 are realistic for this scaling relation, and for this scenario the potential-dependent switching of the preferred mechanistic pathway at the volcano apex still holds true (cf. **Figures S4-S5**).

Therefore, we outline the limits of the presented approach in that only in the case of extreme deviations from the scaling relations, mechanistic complexity at the OER volcano apex is not observed (cf. **Figures S6-S7**). The reported conclusions of the main text are yet fully coherent in the case of modest deviations from the scaling relations (cf. **Figures S2-S5**), and this condition is met for most of the experimentally synthesized and theoretically modeled OER materials so far **[5,6]**.

References

[1] Viswanathan, V.; Hansen, H. A. Unifying solution and surface electrochemistry: limitations and opportunities in surface electrocatalysis. Top. Catal. 2014, 57, 215-221.

[2] Calle-Vallejo, F.; Krabbe, A.; Garcia-Lastra, J. M. How Covalence Breaks Adsorption-Energy Scaling Relations and Solvation Restores Them. Chem. Sci. 2017, 8, 124-130.

[3] Exner, K. S. Design Criteria for Oxygen Evolution Electrocatalysts from First Principles: Introduction of a Unifying Material-Screening Approach. ACS Appl. Energy Mater. 2019, 2, 7991−8001.

[4] Exner, K. S. Steering Selectivity in the Four-Electron and Two-Electron Oxygen-Reduction Reactions: On the Importance of the Volcano Slope. ACS Phys. Chem. Au 2023, DOI: 10.1021/acsphyschemau.2c00054.

[5] McCrory, C. C. L.; Jung, S.; Peters, J. C.; Jaramillo, T. F. Benchmarking Heterogeneous Electrocatalysts for the Oxygen Evolution Reaction. J. Am. Chem. Soc. 2013, 135, 16977-16987.

[6] Seh, Z. W.; Kibsgaard, J.; Dickens, C. H.; Chorkendorff, I. B.; Nørskov, J. K.; Jaramillo, T. F. Combining Theory and Experiment in Electrocatalysis: Insights Into Materials Design. Science 2017, 355, eaad4998.